ORIGINAL PAPER

Film-forming Characteristics of Grease in Point Contact under Swaying Motions

Gang Li · Chenhui Zhang · Jianbin Luo · Shuhai Liu ·
Guoxin Xie · Xinchun Lu

Abstract The technique of relative optical interference intensity (ROII) and simple numerical calculations were used to investigate the lubricating behavior of grease lubricant films in the rolling direction under swaying motions (acceleration/deceleration). Experimental results indicate that at a same entrainment velocity of the inlet, the central film thickness under deceleration is larger than that under acceleration. The minimum central film thickness in one swaying cycle does not occur at the moment of zero entrainment, but at the initial period of acceleration. At the moment of zero entrainment, the central film is thicker than its peripheries, and the value of the central film thickness increases with increases in the changing rate of the entrainment velocity. It is thought that the transient behaviors of the grease lubricant film deviate from those in steady state conditions. The profiles of the transient film thickness and the approximate thicknesses of elastohydrodynamic contact in the rolling direction calculated by using a simple numerical method are supported by the experimental results. The numerical method can also be used to explain the behavior of the grease lubricating film under non-steady state conditions.

Keywords Film thickness · Grease lubricant ·
Non-steady state · Swaying motions

G. Li · C. Zhang (✉) · J. Luo · S. Liu · G. Xie · X. Lu
State Key Laboratory of Tribology, Tsinghua University, Beijing
100084, China
e-mail: chzhang@tsinghua.edu.cn

G. Li
e-mail: ligang06@mails.tsinghua.edu.cn

1 Introduction

Grease is used extensively as a lubricant in many mechanical elements, such as ball and roller bearings, gears, and cams. The primary role of the grease lubricant is to form and maintain a lubricating film between two moving surfaces. This lubricating film can reduce friction, prevent wear, protect bearings against corrosion, and act as a seal to prevent the entry of contaminants. The grease lubricant is expected to lubricate effectively in many applications. However, it has complex bulk structures, in contrast to Newtonian liquid lubricants, and it is difficult to predict the thickness of the elastohydrodynamic (EHD) film [1–4]. Thus, an improved understanding of the characteristics of grease lubricant has far-ranging technical and economic significance.

Many views on grease lubricant have been reported [5–7]. Palacios suggested that the bulk grease may lubricate the contact between two moving surfaces [5]. Cann and Lubrecht considered that the lubricating film formed would be determined by the flow balance between inlet replenishment and loss from the contact [6]. Hurley and Cann observed that the thickness of the grease lubricant film increased with increases in the rolling velocity [7]. It has been demonstrated that variations in EHD behavior depend upon base oil viscosity, soap type and concentration, and most importantly, inlet lubricant supply [1]. The mechanism of oil EHD lubrication is now quite well understood, and many equations are available for calculating both central and minimum film thicknesses in EHD contacts [8]. It has also been argued that the thickness of the grease lubricant film can be approximately calculated using its base oil parameters and that the fully flooded film thickness for grease lubricant is 20–60% greater than that of the base oil [7]. However,

most of these understandings of EHD lubrication are restricted to steady state conditions.

In many practical cases, many of the elements in machines operate under non-steady state conditions, such as entrainment velocity, base oil viscosity, pressure viscosity coefficient, and the inlet lubricant supply. Experimental studies on the transient behavior of lubricant films have been performed by Sugimura [9, 10], Kaneta [11], Glovnea, and Spikes [12–14]. Variations in film thickness as a function of time and position, taking a buffering phenomenon into consideration, were investigated by Dowson et al. [15] and Ai et al. [16]. Glovnea and Spikes [17, 18] studied the behavior of EHD lubricated contacts and proposed a theoretical model for the behavior of EHD films subjected to rapid halting. A variation in the film thickness profile over the contact width for any set of kinematic parameters was given by Messé and Lubrecht [19]. However, most of the above investigations were carried out for liquid oils, and the characteristics of grease lubricant under non-steady state conditions are to date far less understood.

In the investigation reported here, we used the technique of relative optical interference intensity (ROII) to investigate the behavior of grease lubricant film under periodic swaying motions with constant acceleration and deceleration. The aim of our study was to gain an understanding of the lubricating properties of the grease lubricant under transient conditions.

2 Experimental Condition

The non-steady state film thickness measurement system using the technique of ROII is shown in Fig. 1. A detailed explanation of the measuring principle can be found in references [20, 21]. It can be seen from Fig. 2 that the roughness value (R_a) of the ball surface is ≤5 nm and that the R_a of the glass disc surface is ≤2 nm. The ball and the disc are loaded together with an applied load of 14 N, which corresponds to a maximum Hertz pressure of 0.423 GPa. The ball is driven by the disc, and the disc is driven by a motor. The tests are carried out in pure rolling. The acceleration and the relevant velocity scheme which was used in the tests are shown in Fig. 3. In order to avoid starvation, a pair of scoops was used to form a grease pool before the entrance of the contact area. The lithium grease was used as lubricant, and its properties are listed in Table 1. The refractive index of the test grease lubricant is 1.435, which was measured by using the Abbe refractometer. All tests were carried out at 25°C.

The measurement system can be used in many systems of non-steady state motions, including acceleration/deceleration, stop/start, and changing loads. In our study, we selected an adjustable frequency camera to measure the
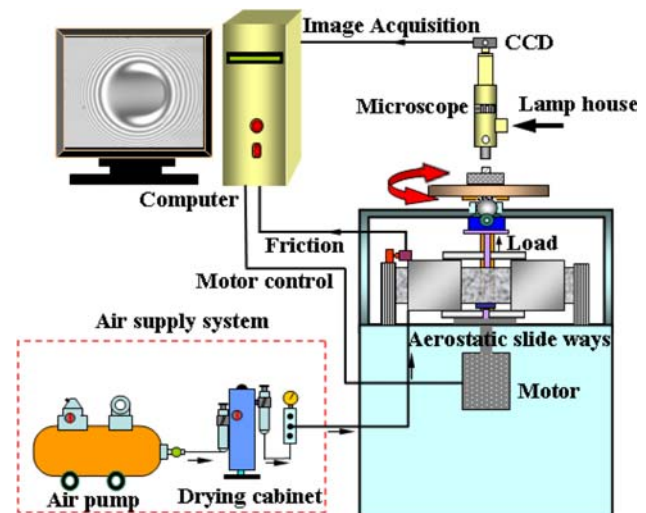

Fig. 1 The scheme of the experimental system. CCD Charge-coupled device
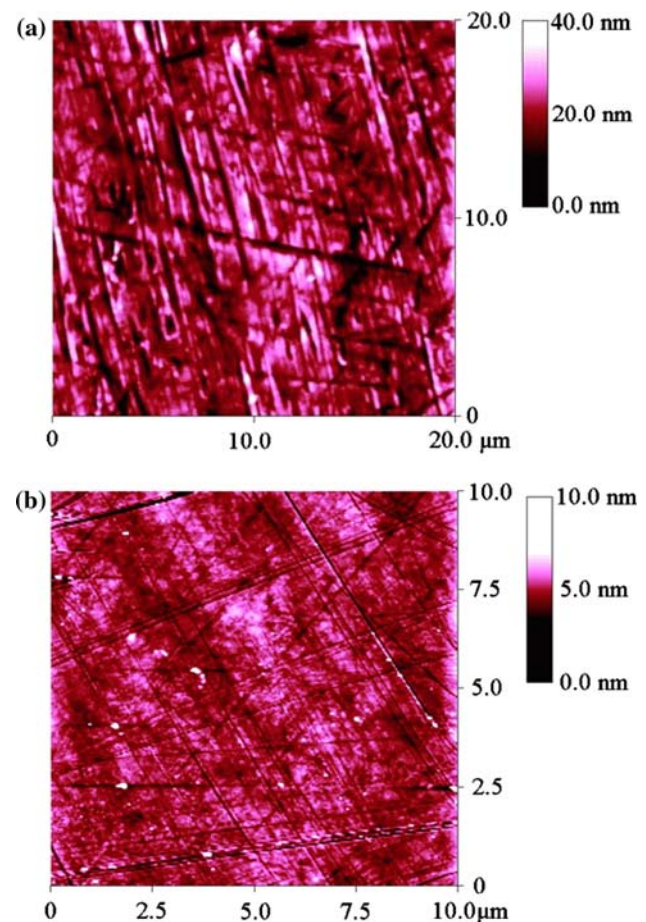
Fig. 2 Surface profile measured by an atomic force microscope (AFM). a Surface profile of the steel ball, $R_a ≤ 5$ nm, b surface profile of the chromium coating, $R_a ≤ 2$ nm

film thickness of the grease lubricant, and the frame frequency was set to 60 frames/s. The camera was synchronized with the disc driving motor by the computer.
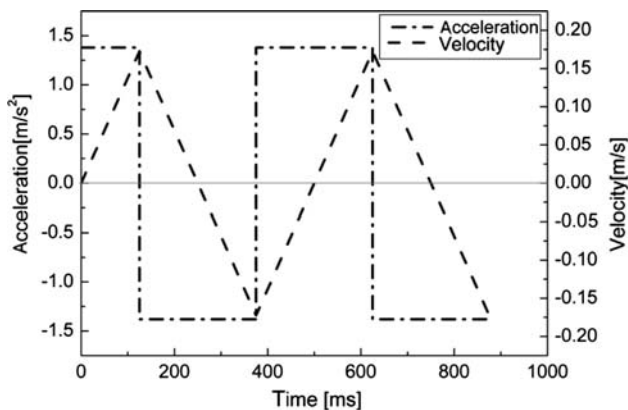
Table 1 Parameters of the grease lubricant in the test

| Temperature (°C)	Soap type	Base oil viscosity (cSt)	Penetration unworked	Penetration worked	Dropping point (°C)
25	Lithium	150	280	280	180

3 Experimental Results

3.1 Variation in Film Shape Around Motion's Reversal

Figure 4 shows a series of interference patterns and the corresponding central contact film profiles at the instants before and after the reversal of motions. The vertical arrows indicate the direction of the changes in the entrainment velocity. During the deceleration period, the entrainment inlet is on the right side of the contact. The moment of zero entrainment corresponds to Fig. 4e, and the constrictive lubricant can be seen in the central contact. After reversal, the initial inlet becomes the outlet, and the motion is under acceleration with the constrictive lubricant passing from left to right across the contact.

Direct visualization of the variation curves are shown in Fig. 5, which presents a succession of film profiles at different entrainment velocities, with Fig. 5a and b corresponding to the deceleration and acceleration periods, respectively. As can be seen in Fig. 5a, at the initial stage of deceleration, the minimum film thickness of the contact area along the rolling direction occurs in the outlet region, and the maximum film thickness in the inlet region. The thickness of the central film decreases with decreasing
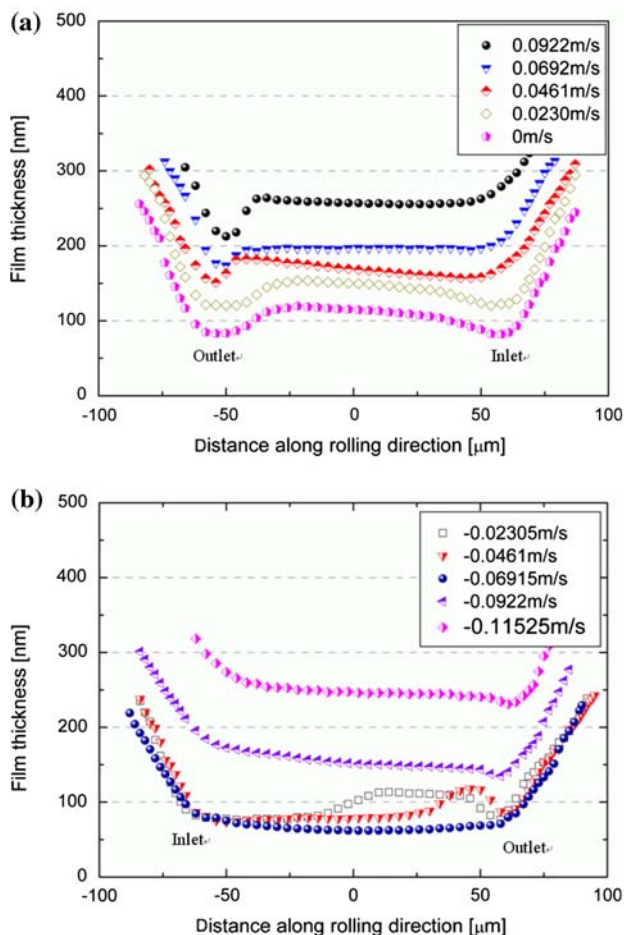
Fig. 4 Interference images and the corresponding film shapes near the moment of zero entrainment
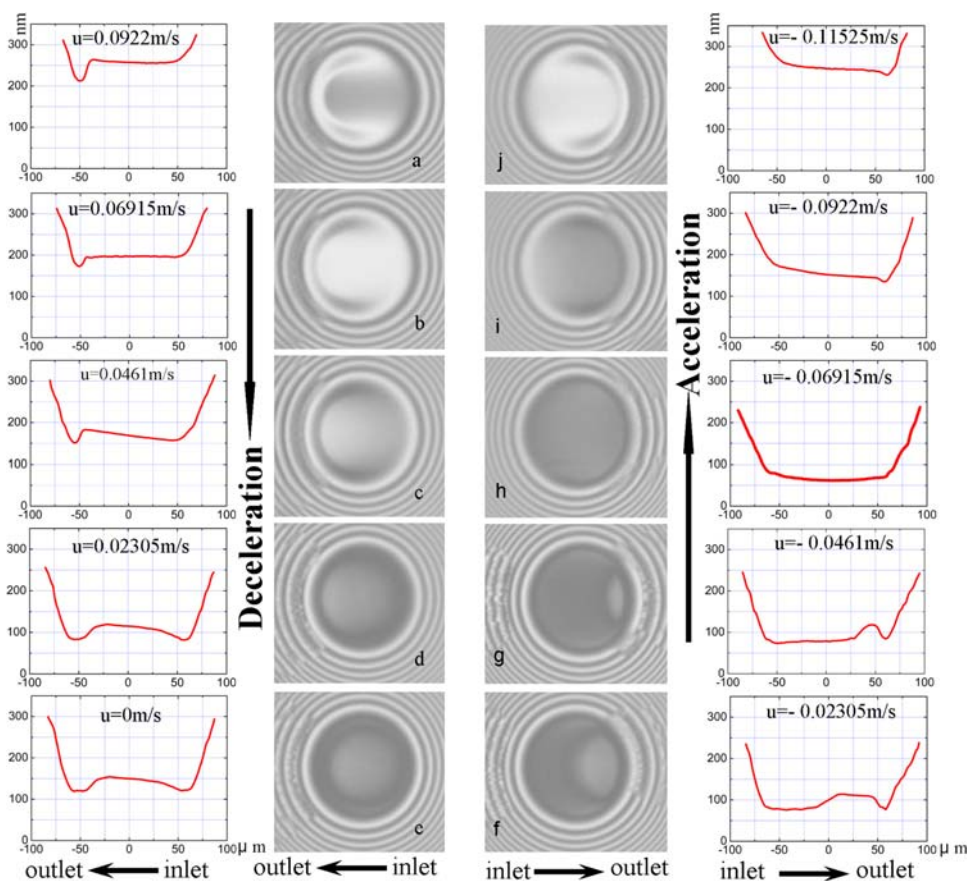
entrainment velocity, and the film thickness of the inlet region decreases more rapidly than that of the outlet region. When the entrainment velocity decreases to 0.0461 mm/s, the maximum film thickness of the central contact occurs at the instant before the outlet restriction, and the film thickness of the inlet region is thinner than that of the outlet region. Around the zero entrainment, the central region of the film is thicker than its peripheries, and the profile of the central film thickness profile in the rolling direction is a "hump". This profile should be due to the fact that the restriction film in central contact needs more time to pass through the peripheral gap under deceleration.

Figure 5b shows the reversal after zero entrainment, when the original outlet of the contact on the left side becomes the inlet. With increasing entrainment velocity, the restriction film in central contact gradually passes through the contact region and moves to the outlet region. With the passing of the restriction film through the central area of the contact, the central film first becomes thicker, then gradually thinner. The minimum central film thickness occurs when the entrainment velocity is −0.06915 mm/s, when the restriction

film has just passed the central contact region. Thereafter, the thickness of the central film increases with increasing entrainment velocity, with the thickness of the film of the inlet region increasing more quickly than that of the outlet region. After the entrainment velocity of −0.0922 m/s, the maximum film thickness occurs near the inlet.
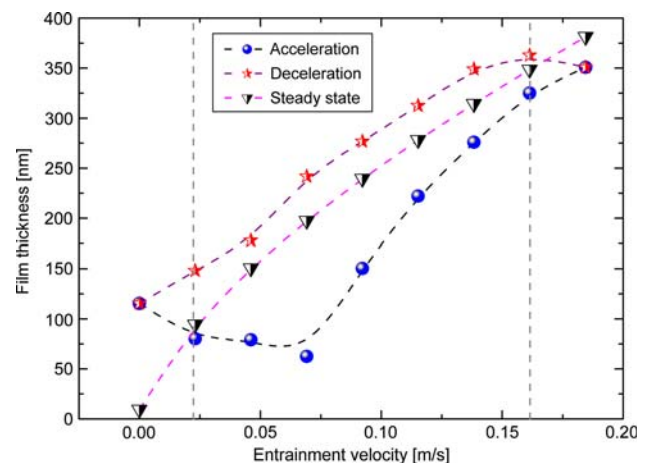
3.2 Variations in the Central Film Thickness During One Swaying Cycle

Figure 6 shows the variation in the central film thickness over one cycle. It can be seen that, at any given entrainment velocity, the film is thicker in the deceleration period than in the acceleration period. Also, the maximum and minimum values of the central film thickness do not coincide with those under the steady state condition. A very clear lag in the film thickness response is shown during conditions of constant acceleration and deceleration; this result is in agreement with those obtained in previous works [22, 23].

The thickness of the central film first increases slightly and then decreases steadily in the deceleration period, continuing to decrease for a short time even after the beginning of the acceleration. This variation probably reflects the fact that the grease lubricant was effectively trapped in the contact during deceleration to retard the rate of change in film thickness. Consequently, as shown in Fig. 6, the minimum central film thickness in one cycle does not fall below about 60 nm even though the result under the steady state condition corresponds to a film thickness of <10 nm.

3.3 Variation in the Central Film Thickness at the Moment of Zero Entrainment

As shown in Fig. 4, the film profile has the form of a "hump" near the zero entrainment. A similar hump-like

Fig. 5 The variation curves of film thicknesses and film profiles before reversal: **a** deceleration, **b** acceleration

**Fig. 6** Variation in the thickness of the central film during one cycle
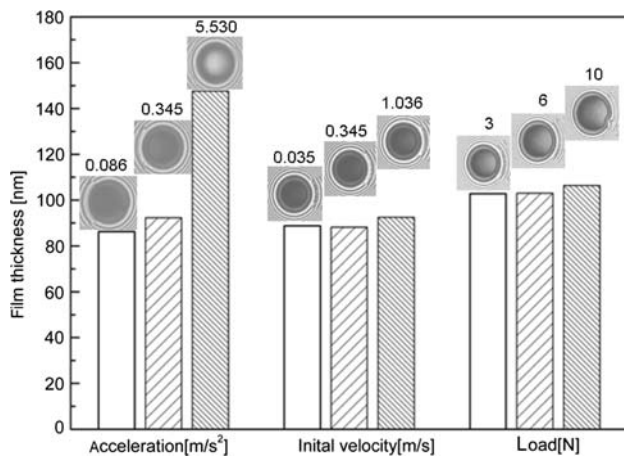
Fig. 7 Effects of variations in experimental parameters on the central film thickness at the moment of zero entrainment (parameters acceleration, load, and initial entrainment velocity)

film profile has been observed in a number of experimental and numerical investigations under transient conditions [11, 12, 24]. Some parameters, such as load, base oil viscosity, the value of acceleration/deceleration, and inlet lubricant supply, have significant effects on central film thickness. In order to study the influence of the change of deceleration, load, and initial velocity on the central film thickness at the moment of zero entrainment, we performed a number of tests under conditions of sudden halting when the lubricant was fully supplied. Figure 7 shows that the thickness of the central film at the moment of zero entrainment clearly increases with the rate of the change of the increase in entrainment velocity, while the influences of the load and the initial entrainment velocity are negligible. In addition, the hump-like lubricant film is much thicker with increases in the viscosity and the pressure/viscosity coefficient of the lubricant [13].

3.4 The Minimum Film Thickness During One Swaying Cycle

In practice, the ratio of the minimum film thickness and the composite roughness is a very important parameter by which to assess the lubrication state between the two surfaces. Under steady motion, the minimum film thickness always occurs at two symmetric points in the horseshoe restriction [25]. Many factors can affect film thickness for the grease lubricant under transient motions. Therefore, the position of the occurrence of the minimum film thickness can be confirmed. As mentioned above, the minimum central film thickness occurs at the instant after the zero entrainment in one cycle. As shown in Fig. 8, the minimum film thickness occurs at the sides of the contact region, transverse to the rolling direction, at the moment of the minimum central film thickness in one cycle. The minimum
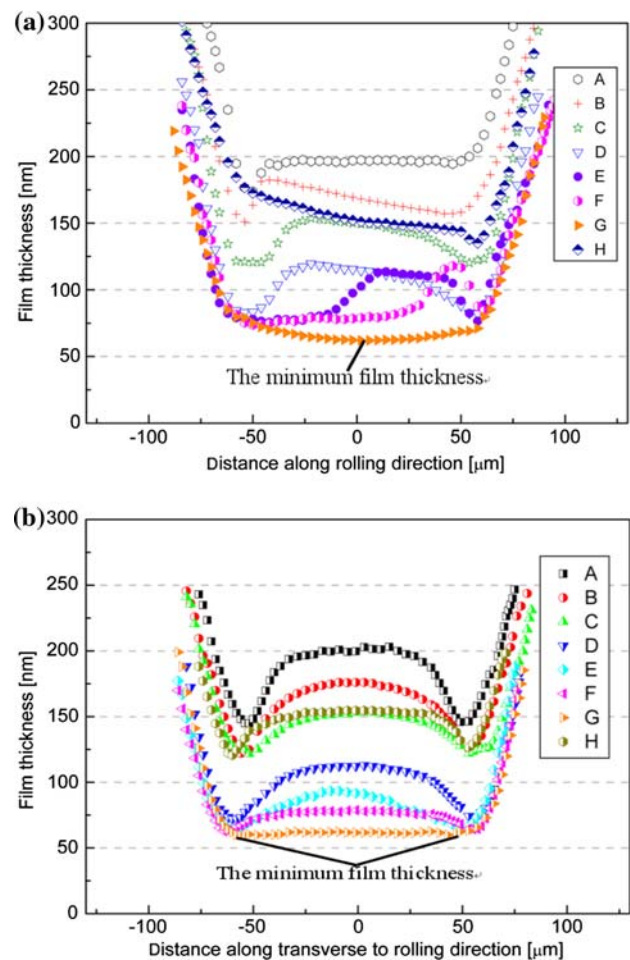
Fig. 8 The film thicknesses in the rolling direction and the transverse direction near zero entrainment. A 69.2 mm/s, B 46.1 mm/s, C 23.1 mm/s, D 0 mm/s, E −23.1 mm/s, F −46.1 mm/s, G −69.2 mm/s, H −92.2 mm/s

film thickness is also slightly lower than the minimum central film thickness.

4 Discussion

Some explanations for the behaviors of film thickness and the film profile under non-steady state motions have been given in the literature. Hydrodynamic effect and squeeze film effect play important roles in the formation and retention of the lubricant film [23, 26, 27].

4.1 The Influence of Hydrodynamic Effect on the Behavior of the Grease Lubricant Film

The fully flooded film thickness for the grease lubricant is greater than that of the corresponding base oil due to an increase in the effective viscosity of the grease lubricant caused by the thickener. The widely accepted practice for

estimating grease lubricant performance is to use the base oil properties to calculate the expected film thickness level. One of the factors determining EHD film thickness is the lubricant viscosity in the inlet region [28]. Kauzlarich and Greenwood [29] assumed a whole grease flow and applied the Herschel–Bulkley model to obtain the inlet viscosity as expressed by:

$$\eta_G = \eta_{BO}(1 + B\phi) \tag{1}$$

where η_G is the viscosity of the fully sheared grease, η_{BO} is the viscosity of the base oil, B is a constant (taken as 2.5 [30]), and ϕ is the volume fraction of soap.

The film thickness of the grease lubricant under the steady state condition can be calculated using Hamrock–Dowson equations [28], which can be given as:

$$h_c = 1.899\alpha^{0.53} \frac{(u\eta_G)^{0.67} R'^{0..397}}{E'^{0.073} W^{0.067}} \tag{2}$$

$$h_{min} = 1.791\alpha^{0.49} \frac{(u\eta_G)^{0.68} R'^{0..393}}{E'^{0.117} W^{0.073}} \tag{3}$$

where h_c is the central film thickness, h_{min} is the minimum film thickness in the rolling direction, u is the entrainment velocity, α is the base oil pressure/viscosity coefficient, R' is the radius of the ball, W is the applied load, and E' is the reduced Young's modulus of the two contacting solids defined by $E' = 2\left((1 - v_1^2)/E_1 + (1 - v_2^2)/E_2\right)$, where v_I is Poisson's ratio for material I and E_I is the Young's modulus of material I.

This part is to give a method by which to estimate the film thickness and the film profile of the grease lubricants in point contacts—for constant acceleration/deceleration. The method is based on the following assumptions: (1) the local film thickness is generated in the inlet, and (2) then transported through the contact region without being altered [28, 31]. Consequently, the film thickness of each point in the Hertzian contact region along the rolling direction can be calculated using the entrainment velocity of each corresponding position passing the inlet. The inlet film thickness at a given time instant may be considered as the steady state film thickness.

In this method, x is the coordinate along the entrainment direction, and x_I is the coordinate of the position of the lubricant molecule just passing the inlet at time instant t_I. According to the above assumptions, the film thickness of coordinate x_I at time instant t is proportional to the entrainment velocity u_I at time instant t_I. The domain of the solution for the film profile is taken from the Hertzian contact inlet, $x = -b$, and the Hertzian contact outlet, $x = b$, where b is the Hertzian contact radius. Assuming that the acceleration is small, one can consider that the test conditions are quasi-steady state. If $a = \partial u/\partial t$ is the acceleration, when $u - \sqrt{u^2 - 4ab} \approx 0$, the test condition can be regard as quasi-steady state. Under this condition,

the prediction using the classical equations will provide accurate results. However, if $u - \sqrt{u^2 - 4ab} \gg 0$, dynamical effects will become important.

In order to agree with the test conditions, the transient condition is the swaying motion and the acceleration a is constant. Thus, the entrainment velocity is considered to be a linear function of time, as shown in Fig. 3. Under transient conditions, the entrainment velocity changes constantly. The following expression describes the entrainment velocity of the inlet:

$$u(t) = u_0 + at \quad t \geq 0 \tag{4}$$

where $u(t)$ is the entrainment velocity at the time instant t, u_0 is the initial entrainment velocity, during acceleration, $u_0 = u_{0a} = 0$, during deceleration, $u_0 = u_{0d} = aT$, where T is the time under deceleration.

If the inlet is on the left side of the contact, where $x = -b$, the distance between the x_I molecule and the inlet is $x_I + b$. If the inlet is on the right side of the contact, where $x = b$, the distance between the x_I molecule and the inlet is $b - x_I$. Under acceleration, if $t \geq 2\sqrt{\frac{b}{a}}$ or under deceleration, if $t \geq \frac{u_{0d}}{a} - \sqrt{\left(\frac{u_{0d}}{a}\right)^2 - 4\frac{b}{a}}$, the entrainment velocity u_I at time instant t_I is called the entering velocity of the oil molecule x_I. The entering velocity can be expressed by Eqs. 5 or 6.

$$u_I = \sqrt{(u(t))^2 - 2a(x_I + b)} \quad \text{(inlet on the left side)} \tag{5}$$

$$u_I = \sqrt{(u(t))^2 - 2a(b - x_I)} \quad \text{(inlet on the right side)} \tag{6}$$

Under acceleration, $a \geq 0$. When $0 \leq t \leq 2\sqrt{\frac{b}{a}}$, if the inlet is on the left side and $x_I + b \leq \frac{1}{2}at^2$, or if the inlet is on the right side and $b - x_I \leq \frac{1}{2}at^2$, the entrainment velocity u_I at time instant t_I can be expressed by Eqs. 5 and 6. When $0 \leq t \leq 2\sqrt{\frac{b}{a}}$, if the inlet is on the left side and $x_I + b \geq \frac{1}{2}at^2$, or if the inlet is on the right side and $b - x_I \geq \frac{1}{2}at^2$, the entrainment velocity u_I at time instant t_I can be expressed by Eqs. 7 or 8

$$u_I = \sqrt{a(b - x_I + a^2t^2)} \quad \text{(inlet on the left side)} \tag{7}$$

$$u_I = \sqrt{a(b + x_I + a^2t^2)} \quad \text{(inlet on the right side)} \tag{8}$$

Under deceleration, $a \leq 0$, when $0 \leq t \leq \frac{u_{0d}}{a} - \sqrt{\left(\frac{u_{0d}}{a}\right)^2 - 4\frac{b}{a}}$, if the inlet is on the left side and $x_I + b \leq u_{0d}t - \frac{1}{2}at^2$, or if the inlet is on the right side and $b - x_I \leq u_{0d}t - \frac{1}{2}at^2$, the entrainment velocity u_I at time instant t_I can be expressed by Eqs. 5 and 6. When $0 \leq t \leq \frac{u_{0d}}{a} - \sqrt{\left(\frac{u_{0d}}{a}\right)^2 - 4\frac{b}{a}}$, if the inlet is on the left side and $x_I + b \geq u_{0d}t - \frac{1}{2}at^2$, or if the inlet is on the right side and $b - x_I \geq u_{0d}t - \frac{1}{2}at^2$, the entrainment velocity u_I at time instant t_I can be expressed by Eqs. 9 or 10

$$u_I = \sqrt{u_{0d}^2 + 2a\left(x_I + b - u_{0d}t + \frac{1}{2}at^2\right)} \qquad (9)$$

(inlet on the left side)

$$u_I = \sqrt{u_{0_d}^2 + 2a\left(b - x_I - u_{0d}t + \frac{1}{2}at^2\right)} \qquad (10)$$

(inlet on the right side)

According to these assumptions, an approximation of the film thickness profile at the time instant t can be calculated by using u_I. Considering u'' to be the entrainment velocity at the moment of the outlet point passing through the inlet, Eqs. 11 and 12 can be obtained:

$$h(x_I, t) = K_1 u_I^{0.67} \qquad (11)$$

$$h_{min}(t) = K_2 u''^{0.68} \qquad (12)$$

where

$$K_1 = 1.899\alpha^{0.53}\frac{\eta_G^{0.67}R'^{0.397}}{E'^{0.073}W^{0.067}},$$

$$K_2 = 1.791\alpha^{0.49}\frac{\eta_G^{0.68}R'^{0.393}}{E'^{0.117}W^{0.073}}.$$

Figure 9 shows the entering velocity of the Hertzian contact oil molecules under three motion modes (acceleration, deceleration, and constant velocity) at a same entrainment velocity of the inlet. The entering velocity of oil molecules in the Hertzian contact region under acceleration is lower than that under constant velocity, while the entering velocity of oil molecules in the Hertzian contact region under deceleration is higher than that under constant velocity. According to Eqs. 11 and 12, the film profiles can be obtained as shown in Fig. 10. The film profiles are similar to the test results shown in
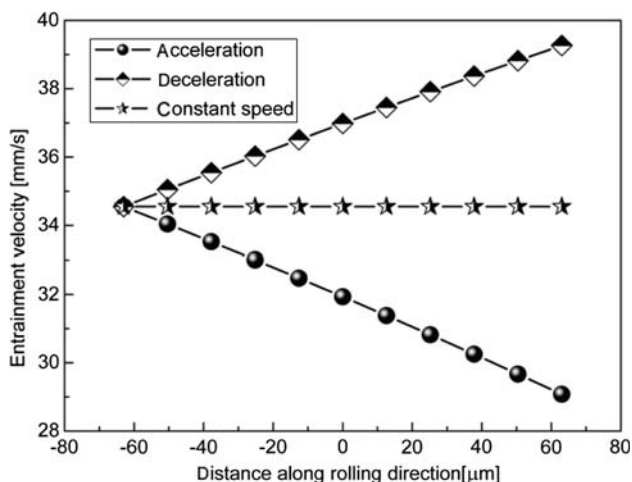
Fig. 9 The entering velocity of the Hertzian contact oil molecules for different accelerations at the same inlet entrainment velocity ($a > 0$, $a < 0$ and $a = 0$)
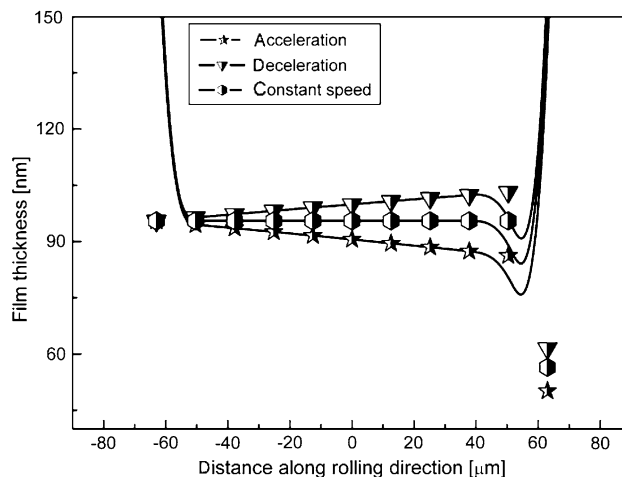

Fig. 10 Comparison of the film thickness profiles and film thickness values under different accelerations ($a > 0$, $a < 0$, and $a = 0$)

Fig. 5. At a same entering velocity, the central film thickness under deceleration is higher than that under acceleration, and this characteristic is similar to that of the test results shown in Fig. 6.

4.2 The Influence of Squeeze Film Effect on the Variation in Film Thickness

The variation in the entrainment quantity of lubricant molecules is the root of the changes in film thickness. All transient tests combine transient hydrodynamic effect and squeeze motion, which is similar to the case shown in Fig. 11, in which the squeeze film effect is like a damper. The squeeze film effect connected to the film thickness variation over time is always present. Under transient conditions, changes in the thickness of the film arise from variations in the entrainment quantity of lubricant molecules; the ball and the disk approach or depart, resulting in the squeeze film effect, with the squeeze film effect subsequently retarding changes in the film thickness.
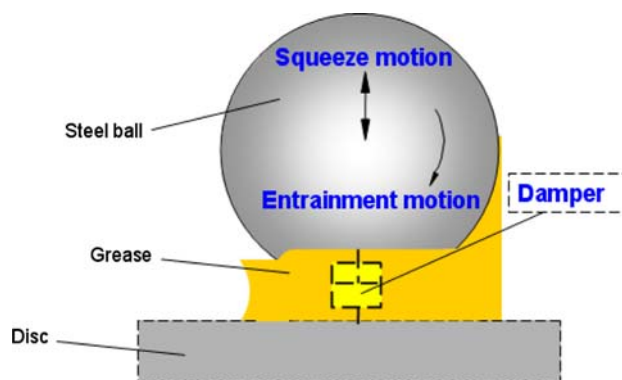
Fig. 11 A schematic diagram of the squeeze film effect

At the beginning of the cycle, with the velocity of the entraining motion increasing, the squeeze film effect works as a separation effect and retards increases in the film thickness, so that the thickness of the film is less than that of the corresponding stationary result. With the velocity of the entraining motion decreasing, the squeeze film effect works as an approaching effect and retards decreases in the film thickness, so that the thickness of the film greater than that of the corresponding stationary result.

At the end of the cycle, due to the decrease in the velocity of the entraining motion ,the entrainment velocity approaches zero, and the squeeze film effect play a major role. The contiguous bodies in the contact area undergo convergence and form a hump profile in the central part of the Hertzian contact region, which can be seen in Fig. 5 at the moment of zero entrainment. This effect has been observed experimentally under pure squeeze motion by Safa and Gohar [32] and Dowson and Jones [28] and also numerically by Dowson and Wang [33]. The squeeze film effect diminishes with decreases in the tested acceleration, and the film thickness tends towards the steady state film behaviors, which has been investigated by Bassani et al. [23].

It can be seen that under transient motion, except for the squeeze film effect, the hydrodynamic effect plays an important role in influencing the behavior of lubricant films.

5 Conclusion

At the moment of zero entrainment during swaying motions, the central film is thicker than its peripheries, and the thickness of the central film increases with increases in the rate of change of the entrainment velocity. The central film thickness of the contact region does not have a minimum value during one cycle at the moment of zero entrainment, but there is a time lag, which depends on the rate of change of the entrainment velocity and the dimensions of the Hertzian contact region. The film thickness of the former outlet region is greater than that of the inlet region at the moment of zero entrainment. However, the film thickness of the former outlet region falls sharply after the resumption of entrainment. At a same entrainment velocity of inlet, the central film thickness under deceleration is greater than that under acceleration. Under transient motions, the squeeze film effect and the hydrodynamic effect are the major factors that influence the behaviors of the grease lubricant films. Experimental results also indicate that the local film thickness is generated in the inlet and then transported through the contact region without being altered. A numerical method has been presented by which to estimate the profiles of the transient film thickness and approximate the thicknesses of the Hertzian contact region in the rolling direction. This method is supported by the experimental results.

References

1. Cann, P.M., Spikes, H.A.: The behaviour of greases in elasto-hydrodynamic contacts. J. Phys. D Appl. Phys. **25**, A124–A132 (1992)
2. Cann, P.M., Doner, J.P., Webster, M.N., Wikstrom, V.: Grease degradation in rolling element bearings. Tribol. Trans. **44**, 399–404 (2001)
3. Cann, P.M., Spikes, H.A.: Film thickness measurements of greases under normally starved conditions. NLGl Spokesman **56**, 21–31 (1992)
4. Zhu, W.S., Neng, Y.T.: A theoretical and experimental study of EHL lubricated with grease. ASME J. Tribol. **110**, 38–43 (1988)
5. Palacios, J.M., Cameron, A., Arizmendi, L.: Film thickness of grease in rolling contacts. Tribol. Trans. **24**, 474–478 (1981)
6. Cann, P.M., Lubrecht, A.A.: An analysis of the mechanisms of grease lubrication in rolling element bearings. Lubr. Sci. **11**, 227–245 (1999)
7. Hurley, S., Cann, P.M.: Starved lubrication of EHL contacts relationship to bulk grease properties. NLGI Spokesman **64**, 15–23 (2000)
8. Hamrock, B.T., Dowson, D.: Ball bearing lubrication: the elastohydrodynamics of elliptical contacts. Wiley, New York (1981)
9. Sugimura, J., Okumura, T., Yamamoto, Y., Spikes, H.A.: Simple equation for elastohydrodynamic film thickness under acceleration. Tribol. Int. **32**, 117–123 (1999)
10. Sugimura, J., Jones, W.R., Spikes, H.A.: EHD film thickness in non-steady state contacts. ASME J. Tribol. **120**, 442–452 (1998)
11. Kaneta, M.: For the establishment of a new EHL theory. Proc. 25th Leeds–Lyon Symp. Tribol. **36**, 25–36 (1999)
12. Glovnea, R.P., Spikes, H.A.: The influence of lubricant upon EHD film behavior during sudden halting of motion. Tribol. Trans. **43**, 731–739 (2000)
13. Glovnea, R.P., Spikes, H.A.: Behavior of EHD films during reversal of entrainment in cyclically accelerate/deceleration motion. Tribol. Trans. **45**, 177–184 (2002)
14. Glovnea, R.P., Spikes, H.A.: The influence of Cam–Follower motion on elastohydrodynamic film thickness. Proc. Leeds–Lyon Symp. Tribol. **39**, 485–493 (2001)
15. Dowson, D., Taylor, C.M., Zhu, G.: A transient elastohydrodynamic lubrication analysis of a cam and follower. J. Appl. Phys. **25**, 313–320 (1992)
16. Ai, X.L., Yu, H.Q.: A numerical analysis for the transient EHL process of a Cam-Tappet pair in I.C. engine. ASME J. Tribol. **111**, 413–417 (1989)
17. Glovnea, R.P., Spikes, H.A.: Elastohydrodynamic film collapse during rapid deceleration. Part I: experimental results. ASME J. Tribol. **123**, 254–261 (2000)
18. Glovnea, R.P., Spikes, H.A.: Elastohydrodynamic film collapse during rapid deceleration. Part II: theoretical analysis and comparison of theory and experiment. ASME J. Tribol. **123**, 262–267 (2000)
19. Messé, S., Lubrecht, A.A.: Transient elastohydrodynamic analysis of an OHC cam/tappet contact. Proc. IMechE. J. Eng. Tribol. **214**, 415–425 (2000)

20. Luo, J.B., Wen, S.Z., Huang, P.: Thin film lubrication. Part I. Study on the transition between EHL and thin film lubrication using a relative optical interference intensity technique. Wear **194**, 107–115 (1996)

21. Xie, G.X., Luo, J.B., Liu, S.H., Zhang, C.H., Lu, X.C.: Micro-bubble phenomenon in nanoscale water-based lubricating film induced by external electric field. Tribol. Lett. **29**, 169–176 (2008)

22. Ciulli, E.: Time and frequency domain analysis of experimental EHL transient conditions data. Proceedings of the 11th Nordic Symposium on Tribology. Nordtrib, pp. 575–584 (2004)

23. Bassani, R., Ciulli, E., Stadler, K., Carli, M.: Lubricated non-conformal contacts under steady state and transient conditions. Proceedings of the AIMETA General Conference. Firenze University Press, Florence (2005)

24. Wedeven, L.D.: Traction and film thickness measurements under starved EHD conditions. Trans. ASME J. Lubr. Tech. **97**, 321–329 (1975)

25. Dowson, D., Higginson, G.R.: A numerical solution to the elastohydrodynamic problem. J. Mech. Eng. Sci. **1**, 6–15 (1959)

26. Dowson, D., Jones, D.A.: Lubricant entrapment between approaching elastic solids. Nature **214**, 947–948 (1967)

27. Vichard, J.P.: Transient effects of the lubrication of Hertzian contacts. J. Mech. Eng. Sci. **13**, 173–189 (1971)

28. Hamrock, B.J., Dowson, D.: Isothermal elastohydrodynamic lubrication of point contacts. Part III: fully flooded results. ASME J. Tribol. **99**, 264–276 (1977)

29. Kauzlarich, J.J., Greenwood, J.A.: Elastohydrodynamic lubrication with Herschel-Bulkley model greases. Tribol. Trans. **15**, 269–277 (1972)

30. Mansot, J.L., Terech, P., Martin, J.M.: Structural investigation of lubricating greases. Colloids Surf. **39**, 321–333 (1989)

31. Messé, S., Lubrecht, A.: Approximating EHL film thickness profiles under transient conditions. ASME J. Tribol. **124**, 443–447 (2002)

32. Safa, M.M.A., Gohar, A.: Pressure distribution under a ball impacting a thin lubricant layer. ASME J. Tribol. **108**, 372–376 (1986)

33. Dowson, D., Wang, D.: An analysis of the normal bouncing of a solid elastic ball on an oily plate. Wear **179**, 29–37 (1994)